Title: Coupled functional physiological phenotyping and simulation model to infer the transpiration sensitivity traits and its implications for transpiration ideotype design

Author: Ting Sun[1,2#], Rui Cheng[3#], Yudong Sun[3], Rujia Jiang[1], Zhuoyi Wang[1], Pingping Fang[1], Xinyang Wu[1], Kang Ning[1], Pei Xu[1,2*]

Authors' affiliation: [1] College of Life Sciences, China Jiliang University, Hangzhou 310018, P.R. China; [2] Key Laboratory of Specialty Agri-product Quality and Hazard Controlling Technology of Zhejiang Province, Hangzhou 310018, P.R. China; [3]Vegetable Research Centre, Huaiyin Institute of Agricultural Sciences of Xuhuai Region in Jiangsu, Huai'an 223001, P.R. China

[#] Equal contribution.

***Correspondence:** Pei Xu, Email: peixu@cjlu.edu.cn

Main text word count: 2990.

Abstract

As agricultural drought becomes more frequent worldwide, it is essential to improve crop productivity whilst reducing the water consumption to achieve a sustainable production. Plant transpiration and water use efficiency (WUE) collectively determine the yield performance, yet it is challenging to balance the two in breeding programs due to still insufficient mechanistic understanding of the traits. Here we developed a method of quantifying the genotype-specific traits reflecting sensitivity of transpiration to radiation (Rad) and vapor pressure deficit (VPD) under evolving developmental stage and water availability ($S_{Tr\text{-}Rad}$ and $S_{Tr\text{-}VPD}$). Our method takes advantages of the state-of-the-art functional physiological phenotyping (FPP) and the principle of inversely using simulation models. We revealed the genotypic difference of $S_{Tr\text{-}Rad}$ and $S_{Tr\text{-}VPD}$ in three watermelon accessions, the dramatic change in each of them across the treatment phases, and the quantitative impacts of them on dynamic WUE patterns. Based on our findings, a general principle for transpiration ideotype design is proposed, which highlights the benefits of lowering $S_{Tr\text{-}VPD}$ to increase WUE and increasing $S_{Tr\text{-}Rad}$ to offset the decline of Tr. FPP-enabled phenomic selection will help screen for elite crops lines with desired transpiration sensitivities.

Introduction

Global farming land area subject to drought is increasing due to the enhanced evapotranspiration associated with increased temperature, net radiation and decreased relative humidity (IPCC, 2021). Improving crop productivity, particularly under deficit water condition, is essential to safeguard food security under the context of global climate change. Stomata is the gateway of both water efflux (transpiration) and CO_2 intake (assimilation). The plant transpiration rate (Tr) and the ratio of CO_2 assimilation to Tr, which is known as water use efficiency (WUE), collectively determine biomass production and yield (Steduto et al., 2012; Vadez et al., 2014). Large efforts are being devoted to developing drought-resistant crops by adopting a strategy of restricting stomatal closure and thereby water loss; however, a tradeoff between increased WUE and decreased total transpiration as a consequence of stomatal restraint has long impeded breeding for agronomically useful varieties (Dalal et al., 2019). Previous studies have stressed that high-WUE crops usually had a smaller leaf area index (LAI), shorter development stage and thus lower Tr and carbon assimilation (Blum, 2005, 2009).

WUE can change with the pattern of Tr within a day even if the daily cumulative Tr remains unchanged (Taylor et al., 1983; Vadez et al., 2014; Ghanem et al., 2020). Sinclair and Vadez (2012) decoded daily WUE as a function of VPD weighted by diurnal Tr, implying the feasibility of selecting high-WUE varieties by harnessing genotypic variations in the dynamic Tr profile. It has been confirmed that restricted maximum Tr at noon under high VPD could increase the WUE and yield of maize (Jafarikouhini et al., 2022), sorghum (Sinclair et al., 2005) and soybean (Sinclair et al., 2010). Mechanistically, Tr is not only governed by internal factors such as leaf area index (LAI) and structure (e.g. cuticle thickness, stomata number), but external factors including temperature, relative humidity, light intensity, wind speed and soil water availability (Kubota, 2020). The interaction between Tr and the environment confounds phenotypic selection for Tr. According to Pieruschka et al. (2010), transpiration is mainly controlled by the diffusion gradient of water vapor inside and outside the stoma

driven by VPD, and internal evaporation driven by latent heat from Rad. Since the diurnal patterns of Rad and VPD are inconsistent (Gosa et al., 2019), the sensitivities of Tr to VPD and Rad would have a strong impact on the dynamic Tr profile. Simulation models, which combine many biological functional hypotheses in mathematical frameworks, describe the development of plant traits as a consequence of environmental and genetic interaction (Génard et al., 2016). Several simulation models for Tr have been established (Katsoulas and Stanghellini, 2019). Recently, simulation models have found their new use in inferring parameters representing genotype-specific traits or "hidden traits" that are not intuitively extractable from the measured phenotypes. Such an approach is referred to as "inverse modeling" (Chenu et al., 2017).

Compared to morphological traits, plant physiological traits are notoriously difficult to phenotype. The emerging functional physiological phenotyping (FPP) has offered revolutionary paths for phenotyping plant water relations (Xu et al., 2015; Halperin et al., 2017; Li et al., 2020). One of such platforms named "Plantarray" allows for high-resolution (every 3 minutes), non-destructive, simultaneous and continuous recording of meteorological variables and physiological traits such as diurnal Tr and daily biomass gain based on the lysimeter principle. The acquired massive dynamic data from the soil-plant-atmosphere continuum provides unprecedent opportunities for deeply understand the mechanisms of plant water relations. Here, we report the quantification of the genotype-specific dynamic traits of "Tr sensitivity to Rad/VPD" ($S_{Tr\text{-}Rad}$ and $S_{Tr\text{-}VPD}$) by coupling FPP and the modified Penman–Monteith model (Medrano et al., 2005; Jo and Shin, 2021). The implications for transpiration ideotype design are discussed.

Results and discussion

Inferred sensitivity of Tr to Rad/VPD through inverse modeling

Using the Plantarray system, diurnal Tr of three watermelon accessions (Fig 1a) and the relevant environmental parameters for calculation of Rad and VPD were nicely obtained at a 3-min resolution, which showed remarkable fluctuations due to the variation of meteorological and soil water conditions (Fig. 2a-e). To disentangle the

intrinsic traits related to sensitivity of Tr to major environmental factors that were hidden within the daily Tr profiles, the modified Penman–Monteith model (Eq. 1) was employed to fit the dynamic Tr with the measured Rad and VPD, as well as the estimated daily LAI (see more in methods):

$$\mathrm{Tr_i} = A(1 - e^{-K\mathrm{LAI_d}})\mathrm{Rad_i} + B\mathrm{LAI_d} * \mathrm{VPD_i} \qquad (1)$$

Two genotype-specific parameters in this model, *A* and *B*, were essentially the $S_{Tr\text{-}Rad}$ and $S_{Tr\text{-}VPD}$, respectively. The fitted transpiration dynamics well reproduced the measured diurnal transpirations, as evidenced by the high correlation (R^2=0.94) between them and the low total root mean square error (RMSE) of only 0.05 g/min, taking the commercial cultivar "JC5" for example (Fig. 1a). $S_{Tr\text{-}Rad}$ and $S_{Tr\text{-}VPD}$ were thus inferred via inverse modeling in a daily step as shown in Fig 1b & c. We conducted Two-way ANOVA for the daily $S_{Tr\text{-}Rad}$ and $S_{Tr\text{-}VPD}$ within each phase of WI, WD and WR, and the result indicated genotypic variation and dramatic change in each of them across the treatment phases ($P<0.01$, Fig. 1b, c). In general, $S_{Tr\text{-}Rad}$ decreased as the water deficit progressed and rapidly recovered when water was resumed (Fig. 1b); $S_{Tr\text{-}VPD}$, however, decreased quickly on the initial days of water deficit, and continued to decrease gradually on the following days until reaching a rather stable level even when irrigation was resumed (Fig. 1c).

$S_{Tr\text{-}Rad}$ and $S_{Tr\text{-}VPD}$ influenced dynamic WUE patterns

To interrogate the impact of different diurnal Tr (as a consequence of varied $S_{Tr\text{-}Rad}$ and $S_{Tr\text{-}VPD}$) on daily WUE and biomass gain, we extended Sinclair and colleagues' model (Eq. 2), a theoretical expression of WUE (Sinclair et al., 1984; Sinclair and Ghanem, 2020), to the FPP data for dynamic WUE calculation (Eq. 3):

$$\mathrm{WUE} = \frac{K_\mathrm{d}}{\mathrm{VPD_d}} \qquad (2)$$

$$\mathrm{WUE_e} = \frac{\int \mathrm{k_d Tr_i} / \mathrm{VPD_i}}{\int \mathrm{Tr_i}} \qquad (3)$$

The daily estimated WUE (WUE_e, g DW/g H_2O) calculated by Eq.3 based on the Tr and VPD continuously acquired by the system, was found to fluctuate across the course of the experiment and varied significantly by genotype (Fig. 3a). During the WI phase,

WUE (g FW/g H_2O) within this period could be measured based on traditional method, i.e., accumulated daily transpiration dividing by accumulated biomass gain. The measured WUE based on fresh weight returned similar result of genetic difference to estimated WUE_e based on dry weight (Fig. 3b). Among the three genotypes, the WUE_e of "HA" averaged over all three phases was the highest, followed by "JC5" and "PI296341-FR" (Fig. 3a, Fig. S1), in accord with the empirical knowledge that wild varieties tend to possess a higher level of drought resistance by sacrificing more biomass production (Kawasaki et al., 2000). "HA" possessed the highest WUE across all phases, in particular the late WD stage. This genotype exhibited high $S_{Tr\text{-}Rad}$ only at the WD phase and remarkedly low $S_{Tr\text{-}VPD}$ particularly at the WI stage (Fig. 1b & c).

We next calculated higher-resolution (hourly) WUE and biomass gain according to Eq. 3 and Eq. 4:

$$\text{Biomass gain} = \frac{\int K_{\mathrm{d}} \mathrm{Tr_i}}{\mathrm{VPD_i}} \qquad (4)$$

With these data, we were able to conduct a simulation analysis by artificially advancing the dynamic Tr for 1 hour across a whole day (Fig. 3c), which revealed an increase of daily WUE and biomass gain by 29.9 % and 20.0 %, respectively. The interpretation of this result is straightforward: without sacrificing daily accumulative Tr, more Tr in the low-VPD but high-Rad morning time decreases the integral value of daily VPD weighted by Tr, thus contributing to the increase of whole-day WUE and biomass gain according to Eq. 2. Such relatively small, daily improvement will accumulatively lead to an improved seasonal yield.

Transpiration ideotype design based on $S_{Tr\text{-}Rad}$ and $S_{Tr\text{-}VPD}$

Based on the results above, we propose that an optimized combination of $S_{Tr\text{-}Rad}$ and $S_{Tr\text{-}VPD}$ is important for balanced Tr, WUE, and biomass gain. To more systematically reveal this influence, we conducted simulations with the inputs of 5-day meteorological data from each of the WI and WD phases (Fig. 4a, c) and the artificial combinations of $S_{Tr\text{-}Rad}$ and $S_{Tr\text{-}VPD}$ extremes (i.e., highest parameter A × lowest parameter B, lowest A × lowest B, highest A × highest B, and lowest A × highest B in the model) from the 3

watermelon genotypes averaged over each 5-day course (Fig. 4b, d), where LAI was fixed to 3 to maintain a fair canopy size. Since Rad peaked much earlier than VPD in the morning (Fig. 4a, c), high A and low B resulted in high Tr during the low VPD intervals within a day and consequently a low integrated value of daily VPD weighted by Tr (Eq. 1), leading to high WUE (red line in Fig. 4b, d). In contrast, low A × high B would result in low WUE (green line in Fig. 4b, d). For instance, during the WD stage, "HA" carrying significantly higher A and lower B had the highest WUE_e, while PI296341-FR carrying the lowest A and highest B showed the lowest WUE_e (Fig. 1b, Fig. 3b & c).

We predicted the biomass gain of different combinations as shown in Fig 4b, d. During the WI phase, highest A × highest B and lowest A × highest B both resulted in much larger Tr, which produced approximately double the biomass gain compared to the remaining combinations despite their lower WUE (Fig. 4b). While during the WD phase, the highest A × highest B still obtained the highest biomass gain benefitting from the highest Tr (blue line in Fig. 4d), but the highest A × lowest B obtained a second highest biomass gain. Therefore, by considering both WUE and Tr, we put forward the following principles for transpiration ideotype design: in the well-irrigated agricultural areas, crop genotypes with high $S_{Tr\text{-}Rad}$ and high $S_{Tr\text{-}VPD}$ is favorable by producing superior yield; in the arid agricultural areas where water-saving is a necessity, genotypes with high $S_{Tr\text{-}Rad}$ and low $S_{Tr\text{-}VPD}$ is desired for its marvelously reduced transpiration yet still considerable yield; in the intermittent drought-prone areas where irrigation and water shortage alternate, genotypes showing strong plasticity in $S_{Tr\text{-}Rad}$ and $S_{Tr\text{-}VPD}$ that are suited to the optimized balance of yield and water consumption will be desired.

Conclusions

We demonstrate that dynamic (daily to hourly or even instantaneous) WUE can be estimated by coupling existing WUE models with the dynamically recorded transpiration and VPD from high-throughput FPP, which breaks the bottleneck of dynamic WUE acquisition. We further demonstrate that daily WUE is affected by the

179 diurnal transpiration pattern of a plant, which is tightly linked to the genotype-
180 dependent sensitivity of Tr to Rad and VPD. A quantitative approach was developed to
181 infer these transpiration sensitivity parameters. We propose that it is beneficial to
182 increase WUE by lowering $S_{Tr\text{-}VPD}$ while offsetting its negative impact on Tr by
183 increasing $S_{Tr\text{-}Rad}$. Although in previous studies high-WUE crops selected by carbon
184 isotope discrimination generally failed to match the demand of luxuriant growth (Blum,
185 2005, 2009), the high-WUE trait is not necessarily linked to growth limitation
186 (Marguerit et al. (2014), which lays the foundation for synergistic improvement of
187 WUE and yield. FPP-enabled phenomic selection will help catch the desired elite
188 individuals from enormous germplasm lines, e.g. those with substantially high $S_{Tr\text{-}Rad}$
189 under both well-watered and water scarcity conditions.

190 **Materials and methods**

191 **Plant materials and experimental design**

192 Three genotypes of watermelon, i.e., a wild watermelon accession "PI-296341-FR"
193 (*Citrullus lanatus* var. citroides), a cultivated watermelon variety "Jincheng No. 5"
194 (*Citrullus lanatus* var. lanatus, hereafter JC5) popular in Northwest China, and a
195 drought-tolerant inbred line of *Citrullus lanatus* var. lanatus "HA" were used in this
196 study. The experiments were carried out in the spring and summer seasons of 2021 in a
197 semi-controlled greenhouse (L×W×H: 10m×5m×4m) in Huai'an (119°01′E, 33°35′N),
198 China. One seedling at the three-leaf stage was transplanted per pot
199 (16cm×13cm×18cm, 1.5 L) with Profile Porous Ceramic substrate (diameter: 0.2mm,
200 pH: 5.5±1, porosity: 74, and CEC: 33.6mEq/100g).

201 Four replicates for each genotype were set in a completely randomized design on
202 'Plantarray' (Plant-Ditech, Israel, Fig.2a). This system provides a simultaneous
203 measurement and detailed physiological response profile for plants in each pot (Li et
204 al., 2020). Water and nutrient supplements (Yamazaki nutrient solution) were controlled
205 by the automatic irrigation system of Plantarray. Experiment in each growth season
206 included three treatment periods, i.e., well-irrigation (WI), progressive water deficit
207 (WD) and water recovery (WR). Under the WI and WR phase, nutrient solution was

provided by irrigation for 240 seconds (oversaturated) at 23:00, 1:00, 2:00, and 3:00 of a day, respectively, and no nutrient solution was supplied during the WD stage.

Functional physiological phenotyping (FPP)

The physiological parameters, e.g., Tr (g min^{-1}), daily transpiration (*E*, g d^{-1}), and daily plant growth (PG, g FW d^{-1}) for plant water relations were obtained using the SPAC software implemented in the "Plantarray" system according to the continuously monitored system weight (Fig. 2a & b). PG was determined as the difference of predawn system weight between consecutive days, before which the pots had been saturated irrigated and drained with no bulk water. As each pot on the system was covered with plastic film, soil evapotranspiration was prevented. The whole-plant WUE during the WI period was determined by the ratio between the accumulated PG and *E*.

The air temperature (T_{air}, ℃) and relative humidity (RH, %), photosynthetically active radiation (PAR, μmol m^{-2} s^{-1}) above the canopy, and soil volumetric water content (VWC, m^3 m^{-3}) in each pot were measured by the VP-4, 5TM, and PYR solar radiation sensor (Decagon Devices, Pullman, Wash, USA), respectively (Fig. 2c-e, Fig. S2). VPD (kPa) was calculated according to Halperin et al. (2017).

Transpiration model

A modified Penman–Monteith equation model for greenhouse transpiration (Medrano *et al.*, 2005; Jo & Shin, 2021) was employed to simulate transpiration rate, which is described as the following equation:

$$\lambda \mathrm{Tr_i} = A(1 - e^{-K\mathrm{LAI_d}})\mathrm{Rad_i} + B\mathrm{LAI_d} * \mathrm{VPD_i} \qquad (1)$$

where λ is the vaporization heat of water (J kg^{-1}), Tr_i is the instantaneous transpiration rate, *K* is the light extinction coefficient (0.86), Rad_i is the instantaneous solar radiation (W m^{-2}, converted from PAR), LAI_d is the daily leaf area index (m^{-2} m^{-2}). VPD_i is the instantaneous vapor pressure deficit. The LAI was estimated based on daily transpiration in each experiment unit by considering the individual difference (detailed as follows).

LAI estimation and validation

Step 1, dynamic Tr recorded in a frequency of every 3 minutes across a day was fitted to the observed radiation and VPD, thus optimum *A*, *B*, and LAI in the modified Penman–Monteith equation (Eq. 1) were estimated according to nonlinear least square (NLS) method and trust-region algorithm via the trial version of MATLAB 2018b (MathWorks, Inc., Cambridge, MA, USA). Only daily LAI with robust goodness of fit (adjusted R^2>0.85) were picked for subsequent calculations. Step 2, we checked the accumulated daily transpiration (*E*) measured by Plantarray and the estimated LAI from daily fitting of step 1, where good linear relationship was found between them. Therefore, a constant LAI growth rate per E was estimated for individual experiment units, and then daily LAIs of individual experiment units were re-calculated according to daily measured E and estimated LAI growth rate per E. Step 3, daily parameter *A* and *B* were determined with observed Tr, RAD, VPD and re-calculated LAI during Step 2 for WI, WS, and WR stage, respectively. Parameter fitting was performed also with MATLAB 2018b.

Independent experiment was conducted to verify the aforementioned method, where estimated LAI was compared to the LAI measured by an LA-S leaf area analyzer system (Wanshen Technology Co., Hangzhou, China). The result proved that such approach of LAI estimation was suitable, with a RMSE of only 0.073 between the estimated and measured values (Fig. 5).

Simulation of WUE and biomass gain

The initial definition of WUE considers the resistances to diffusion resulting from stomata, leaf aerodynamic boundary layer, and leaf mesophyll resistance, and can be ultimately simplified to:

$$\mathrm{WUE} = \frac{K_\mathrm{d}}{\mathrm{VPD_d}} \quad (2)$$

where $\mathrm{VPD_d}$ is the mean VPD over a day. K_d is a coefficient that reflects the CO_2 concentration in the stomatal chamber, which has been validated among different crops (Tanner and Sinclair, 1983; Sinclair et al., 1984). The mean value of K_d in Eq 2-4 was estimated as 6.5 kPa according to the method described by Tanner and Sinclair (1983) for the growth period.

To measure WUE over a long period, VPD needs to be integrated over a growth season and weighted by the transpiration over the course (Taylor et al., 1983; Vadez et al., 2014; Ghanem et al., 2020). Applying the same logic to a single day, Sinclair and Vadez (2012) proposed an assumption that the weighting of this component based on the transpiration rate throughout the day leads to the possibility of obtaining altered values if there are genotypic variations in the transpiration profile throughout the day. Therefore, during a computation interval (i), the mean VPD (VPD_i) is weighted for mean transpiration rate (Tr_i) to calculate the estimated WUE (WUE_e) as in the following integrating equation:

$$\mathrm{WUE_e} = \frac{\int K_\mathrm{d}\mathrm{Tr_i}\,/\mathrm{VPD_i}}{\int \mathrm{Tr_i}} \qquad (3)$$

And biomass gain during this period could be estimated as:

$$\text{Biomass gain} = \frac{\int K_\mathrm{d}\mathrm{Tr_i}}{\mathrm{VPD_i}} \qquad (4)$$

Acknowledgments

We thank the supports of National Key Research & Development Program of China (2021YFE19800), the Research & Development Program of Ningbo (2021Z006) and the Key Scientific and Technological Grant of Zhejiang for Breeding New Agricultural Varieties (2021C02066-5, 2021C02067-7).

Figure legends

Figure 1 Simulation of diurnal transpiration by using the modified Penman-Monteith model. a, observed and simulated diurnal variation of transpiration rate during summer-season experiment in 2021, taking an experiment unit of JC5 for instance. The observations and simulations were both 3-min steps. b-c, fitted daily parameter A or $S_{Tr\text{-}Rad}$ (b) and parameter B or $S_{Tr\text{-}VPD}$ (c) by modified Penman-Monteith model during summer-season experiment in 2021. Multiple comparison results among three genotypes (PI296341-FR, JC5, and HA) were shown as mean values with lowercase letters to show statistically significant differences for the well-irrigation (WI), progressive water deficit (WD) and water recovery (WR) phases, respectively.

Figure 2 Parameters of soil–plant–atmosphere continuum monitored by high-throughput phenotyping platform "Plantarray". a, overview of the automated physiological phenotyping array loaded with watermelon seedlings. b, system weights that were recorded every 3 minutes during the experimental course. Shadow areas show the observed variation. The experiment was divided into the well-irrigation (WI), progressive water deficit (WD), and water recovery (WR) phases. c-e, meteorological parameters, i.e., air temperature (T_{air}, ℃, c), relative humidity (RH, %, d), and photosynthetic active radiation (PAR, μmol m^{-2} s^{-1}, e) during the summer-season experiment in 2021.

Figure 3 Measured and estimated water use efficiency (WUE), and estimated biomass gain based on models. a, Dynamic Tr (every 3 minutes), hourly WUE and biomass gain estimated based on models, taking the data from an experiment unit in June 19 for instance. A left-ward shift of dynamic Tr was applied to artificially advance it for 1 h. Corresponding WUE and biomass gain were estimated and shown as dotted lines. b, daily estimated WUE (WUE_e, g DW g^{-1} H_2O) using mechanism models based on continuously recorded transpiration rate and VPD by Plantarray during the summer-season experiment in 2021. Multiple comparison results among three genotypes were shown as mean values with lowercase letters to show statistically significant differences for the well-irrigation (WI), progressive water deficit (WD) and water recovery (WR) phases, respectively. **c**, measured WUE (g FW g^{-1} H_2O) based on accumulated biomass

and transpiration during the summer-season experiment in 2021. Accumulated biomass (g FW) and transpiration (g H_2O) were calculated according to daily biomass gain and daily transpiration measured by "Plantarray" system during WI phase. Accumulated biomass of PI296341-FR, JC5 and HA were fitted to a linear function of accumulated transpiration for individual experiment units, and multiple comparison results among three genotypes were shown.

Figure 4 Diurnal variation of Rad and VPD, and the responsive patterns of simulated Tr to different combinations of parameter A and B. a, c five-day Rad and VPD (normalized to 0-1 scale) recorded at 3-min intervals, which were selected from the well-irrigation (WI, 6.17-6.21, a) and progressive water deficit (WD, 6.25-6.29, c) phase, respectively. The LAI was set to a constant of 3 for all simulations. Mean values of parameters A and B for different genotypes (PI296341-FR, JC5, and HA) were calculated over each 5-day course, and the maxima and minima formed the four combinations as shown in the graph. Mean estimated WUE and biomass gain over 5-day course were denoted as $WUE_{e,5d}$ and $Biomass_{e,5d}$, respectively.

Figure 5 Comparison of estimated and measured leaf area index (LAI). LAI was estimated by the methods described in the "Leaf area index (LAI) estimation" section of SI (shown as lines). At 13,17, 21, 25 and 28 days after transplanting, leaf tissues from 3 experiment units of Plantarray were destructively removed from watermelon plants, respectively. Leaf areas were measure by LA-S leaf area analyzer system (shown as circles). RMSE represents root mean square error.

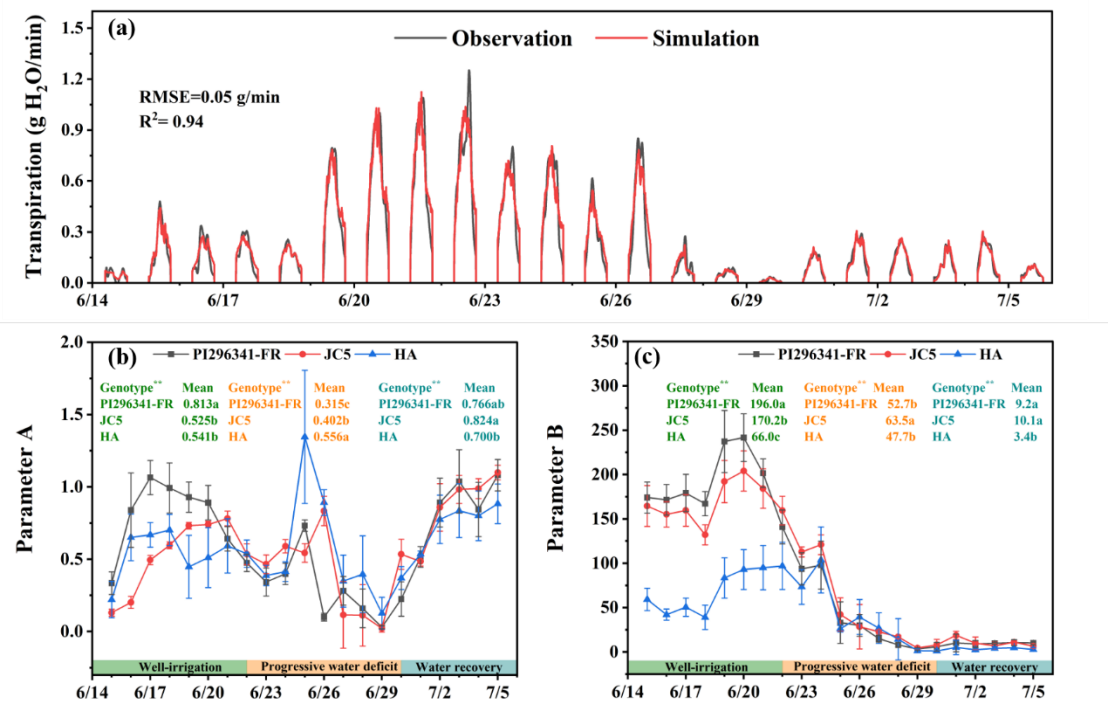

Figure 1 Simulation of diurnal transpiration by using the modified Penman-Monteith model. a, observed and simulated diurnal variation of transpiration rate during summer-season experiment in 2021, taking an experiment unit of JC5 for instance. The observations and simulations were both 3-min steps. b-c, fitted daily parameter A or $S_{Tr\text{-}Rad}$ (b) and parameter B or $S_{Tr\text{-}VPD}$ (c) by modified Penman-Monteith model during summer-season experiment in 2021. Multiple comparison results among three genotypes (PI296341-FR, JC5, and HA) were shown as mean values with lowercase letters to show statistically significant differences for the well-irrigation (WI), progressive water deficit (WD) and water recovery (WR) phases, respectively.

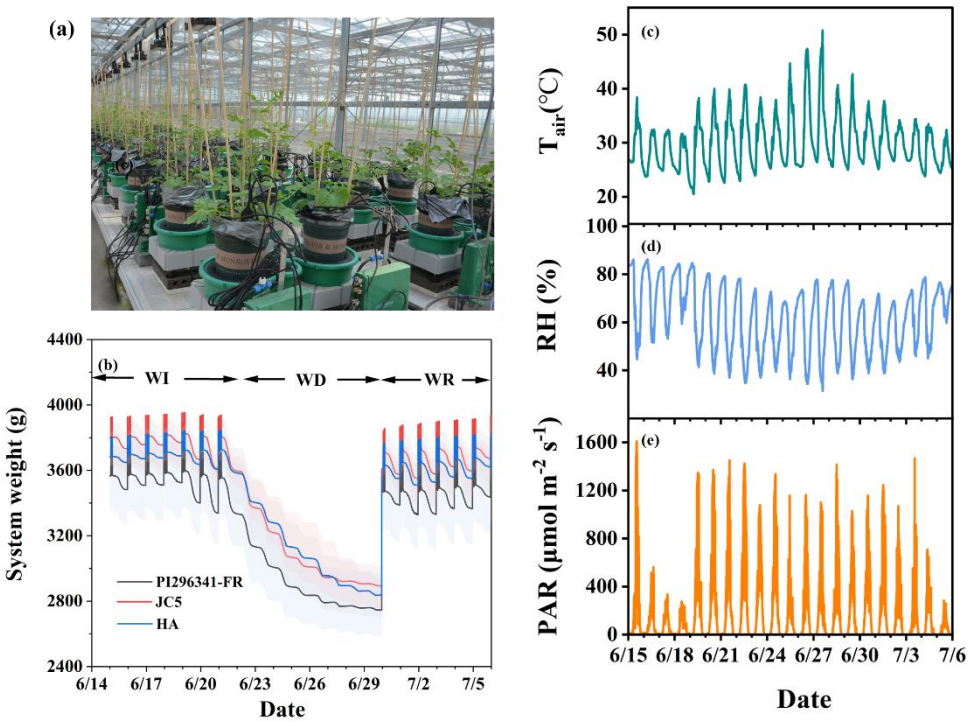

Figure 2 Parameters of soil–plant–atmosphere continuum monitored by high-throughput phenotyping platform "Plantarray". a, overview of the automated physiological phenotyping array loaded with watermelon seedlings. b, system weights that were recorded every 3 minutes during the experimental course. Shadow areas show the observed variation. The experiment was divided into the well-irrigation (WI), progressive water deficit (WD), and water recovery (WR) phases. c-e, meteorological parameters, i.e., air temperature (T_{air}, ℃, c), relative humidity (RH, %, d), and photosynthetic active radiation (PAR, μmol m^{-2} s^{-1}, e) during the summer-season experiment in 2021.

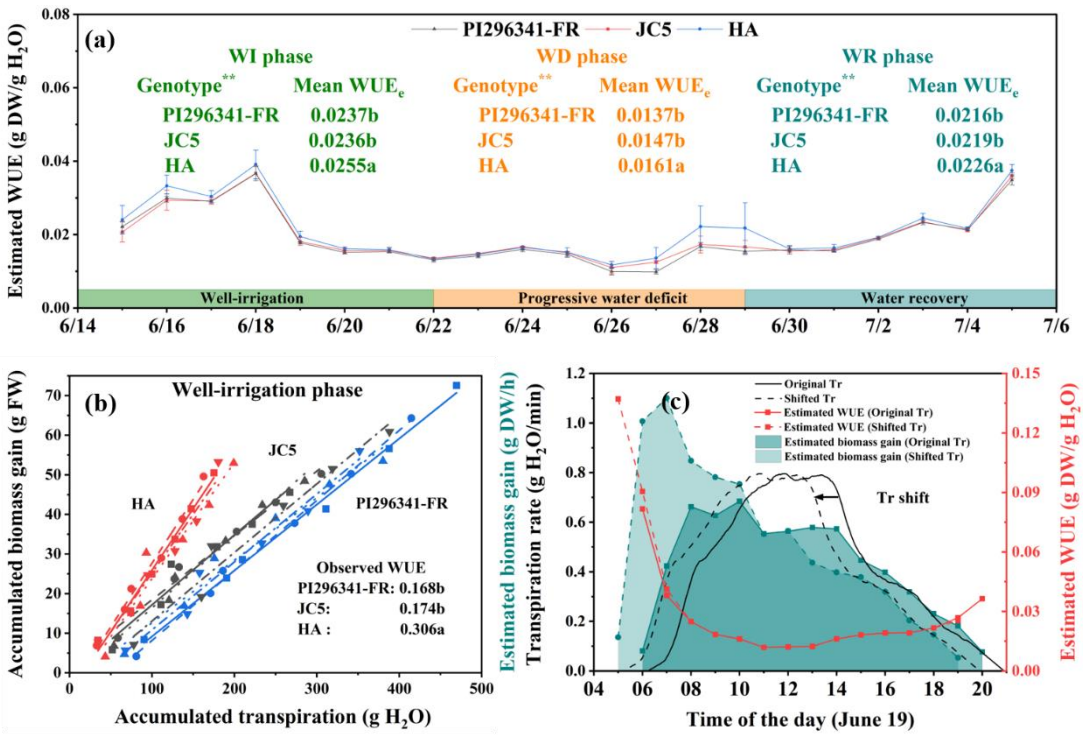

Figure 3 Measured and estimated water use efficiency (WUE), and estimated biomass gain based on models. a, daily estimated WUE (WUEe, g DW g-1 H2O) using mechanism models based on continuously recorded transpiration rate and VPD by Plantarray during the summer-season experiment in 2021. Multiple comparison results among three genotypes were shown as mean values with lowercase letters to show statistically significant differences for the well-irrigation (WI), progressive water deficit (WD) and water recovery (WR) phases, respectively. b, measured WUE (g FW g-1 H2O) based on accumulated biomass and transpiration during the summer-season experiment in 2021. Accumulated biomass (g FW) and transpiration (g H2O) were calculated according to daily biomass gain and daily transpiration measured by "Plantarray" system during WI phase. Accumulated biomass of PI296341-FR, JC5 and HA were fitted to a linear function of accumulated transpiration for individual experiment units, and multiple comparison results among three genotypes were shown. c, dynamic Tr (every 3 minutes), hourly WUE and biomass gain estimated based on models, taking the data from an experiment unit in June 19 for instance. A left-ward shift of dynamic Tr was applied to artificially advance it for 1 h. Corresponding WUE and biomass gain were estimated and shown as dotted lines.

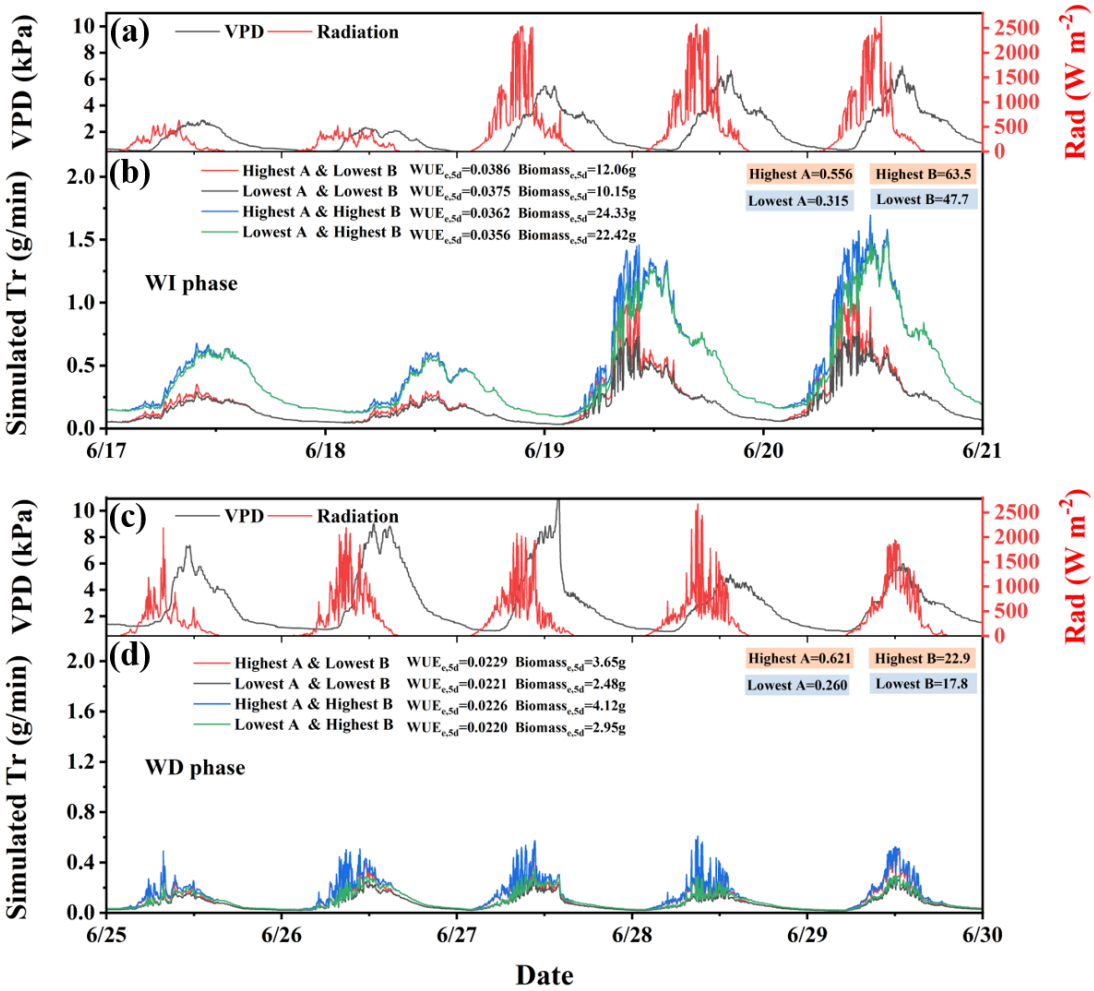

Figure 4 Diurnal variation of Rad and VPD, and the responsive patterns of simulated Tr to different combinations of parameter A and B. a, c five-day Rad and VPD (normalized to 0-1 scale) recorded at 3-min intervals, which were selected from the well-irrigation (WI, 6.17-6.21, a) and progressive water deficit (WD, 6.25-6.29, c) phase, respectively. The LAI was set to a constant of 3 for all simulations. Mean values of parameters A and B for different genotypes (PI296341-FR, JC5, and HA) were calculated over each 5-day course, and the maxima and minima formed the four combinations as shown in the graph. Mean estimated WUE and biomass gain over 5-day course were denoted as $WUE_{e,5d}$ and $Biomass_{e,5d}$, respectively.

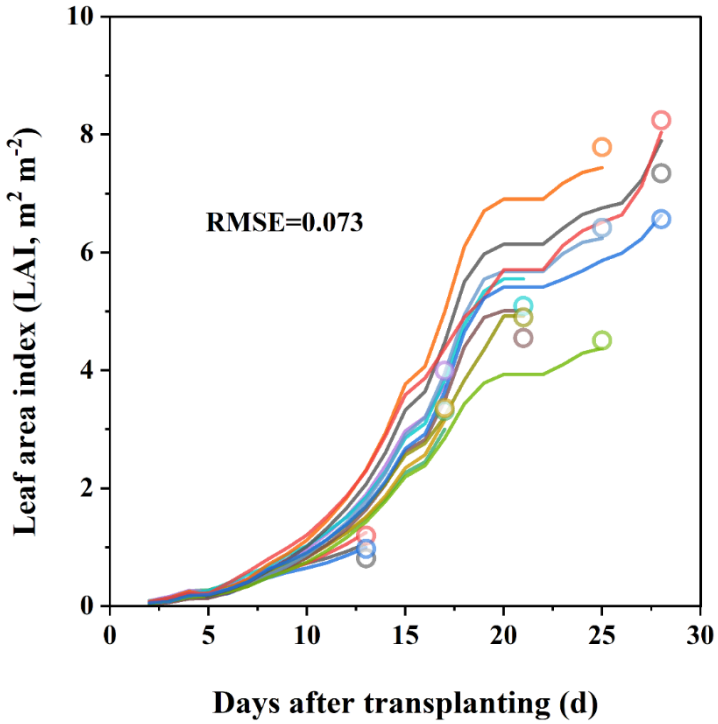

Figure 5 Comparison of estimated and measured leaf area index (LAI). LAI was estimated by the methods described in the "Leaf area index (LAI) estimation" section of SI (shown as lines). At 13,17, 21, 25 and 28 days after transplanting, leaf tissues from 3 experiment units of Plantarray were destructively removed from watermelon plants, respectively. Leaf areas were measure by LA-S leaf area analyzer system (shown as circles). RMSE represents root mean square error.

References

Blum A (2005) Drought resistance, water-use efficiency, and yield potential—are they compatible, dissonant, or mutually exclusive? Australian Journal of Agricultural Research **56:** 1159-1168

Blum A (2009) Effective use of water (EUW) and not water-use efficiency (WUE) is the target of crop yield improvement under drought stress. Field Crops Research **112:** 119-123

Chenu K, Porter JR, Martre P, Basso B, Chapman SC, Ewert F, Bindi M, Asseng S (2017) Contribution of crop models to adaptation in wheat. Trends in Plant Science **22:** 472-490

Dalal A, Bourstein R, Haish N, Shenhar I, Wallach R, Moshelion M (2019) Dynamic physiological phenotyping of drought-stressed pepper plants treated with "productivity-enhancing" and "survivability-enhancing" biostimulants. Frontiers in Plant Science **10:** 905

Génard M, Memmah M-M, Quilot-Turion B, Vercambre G, Baldazzi V, Le Bot J, Bertin N, Gautier H, Lescourret F, Pagès L (2016) Process-based simulation models are essential tools for virtual profiling and design of ideotypes: example of fruit and root. *In* Crop Systems Biology, pp 83-104

Ghanem ME, Kehel Z, Marrou H, Sinclair TR (2020) Seasonal and climatic variation of weighted VPD for transpiration estimation. European Journal of Agronomy **113:** 125966

Gosa SC, Lupo Y, Moshelion M (2019) Quantitative and comparative analysis of whole-plant performance for functional physiological traits phenotyping: New tools to support pre-breeding and plant stress physiology studies. Plant Science **282:** 49-59

Halperin O, Gebremedhin A, Wallach R, Moshelion M (2017) High-throughput physiological phenotyping and screening system for the characterization of plant-environment interactions. The Plant Journal **89:** 839-850

IPCC (2021) Climate change 2021: the physical science basis. Contribution of working group I to the sixth assessment report of the intergovernmental panel on climate change.

Jafarikouhini N, Sinclair TR, Resende MJCS (2022) Limited-transpiration rate and plant conductance in a diverse sweet corn population. Crop Science **62:** 374-381

Jo WJ, Shin JH (2021) Development of a transpiration model for precise tomato (Solanum lycopersicum L.) irrigation control under various environmental conditions in greenhouse. Plant Physiology and Biochemistry **162:** 388-394

Katsoulas N, Stanghellini C (2019) Modelling crop transpiration in greenhouses: different models for different applications. Agronomy **9:** 392

Kawasaki S, Miyake C, Kohchi T, Fujii S, Uchida M, Yokota A (2000) Responses of wild watermelon to drought stress: accumulation of an ArgE homologue and citrulline in leaves during water deficits. Plant and Cell Physiology **41:** 864-873

Kubota C (2020) Growth, development, transpiration, and translocation as affected by abiotic environmental factors. *In* T Kozai, G Niu, M Takagaki, eds, Plant Factory (Second Edition). Academic Press, pp 207-220

Li Y, Wu X, Xu W, Sun Y, Wang Y, Li G, Xu P (2020) High-throughput physiology-based stress response phenotyping: Advantages, applications and prospective in horticultural plants. Horticultural Plant Journal **7:** 181-187

Marguerit E, Bouffier L, Chancerel E, Costa P, Lagane F, Guehl JM, Plomion C, Brendel O (2014) The genetics of water-use efficiency and its relation to growth in maritime pine. Journal of Experimental Botany **65:** 4757-4768

Medrano E, Lorenzo P, Sánchez-Guerrero MC, Montero JI (2005) Evaluation and modelling of

greenhouse cucumber-crop transpiration under high and low radiation conditions. Scientia Horticulturae **105:** 163-175

Pieruschka R, Huber G, Berry JA (2010) Control of transpiration by radiation. Proceedings of the National Academy of Sciences **107:** 13372-13377

Sinclair TR, Ghanem ME (2020) Plant-based predictions of canopy transpiration instead of meteorological approximations. Crop Science **60:** 1133-1141

Sinclair TR, Hammer GL, van Oosterom EJ (2005) Potential yield and water-use efficiency benefits in sorghum from limited maximum transpiration rate. Functional Plant Biology **32:** 945-952

Sinclair TR, Messina CD, Beatty A, Samples M (2010) Assessment across the United States of the benefits of altered soybean drought traits. Agronomy Journal **102:** 475-482

Sinclair TR, Tanner CB, Bennett JM (1984) Water-use efficiency in crop production. Bioscience **34:** 36-40

Sinclair TR, Vadez V (2012) The future of grain legumes in cropping systems. Crop and Pasture Science **63:** 501-512

Steduto P, Hsiao TC, Fereres E, Raes D (2012) Crop yield response to water, Vol 1028. FAO

Tanner CB, Sinclair TR (1983) Efficient water use in crop production: research or re-search? *In* Limitations to efficient water use in crop production. American Society of Agronomy

Taylor HM, Jordan WR, Sinclair TR, Unger PW, Sneed TV, Jordan WR, Jensen R (1983) Limitations to efficient water use in crop production. American Society of Agronomy

Vadez V, Kholova J, Medina S, Kakkera A, Anderberg H (2014) Transpiration efficiency: new insights into an old story. Journal of Experimental Botany **65:** 6141-6153

Xu P, Moshelion M, Wu X, Halperin O, Wang B, Luo J, Wallach R, Wu X, Lu Z, Li G (2015) Natural variation and gene regulatory basis for the responses of asparagus beans to soil drought. Frontiers in Plant Science **6:** 891